Michael A. Malusis,[1] *Charles D. Shackelford,*[2]* *and Harold W. Olsen*[3]

A Laboratory Apparatus to Measure Chemico-Osmotic Efficiency Coefficients for Clay Soils

REFERENCE: Malusis, M. A., Shackelford, C. D., and Olsen, H. W., **"A Laboratory Apparatus to Measure Chemico-Osmotic Efficiency Coefficients for Clay Soils,"** *Geotechnical Testing Journal,* GTJODJ, Vol. 24, No. 3, September 2001, pp. 229–242.

ABSTRACT: A laboratory apparatus for measuring the chemico-osmotic efficiency coefficient, ω, for clay soils in the presence of electrolyte solutions is described. A chemico-osmotic experiment is conducted by establishing and maintaining a constant difference in electrolyte concentration across a soil specimen while preventing the flow of solution through the specimen. The chemico-osmotic efficiency coefficient is derived from a measured pressure difference induced across the specimen in response to the applied concentration difference. The effective diffusion coefficient (D^*) and retardation factor (R_d) of the electrolytes (solutes) also can be determined simultaneously by measuring the diffusive solute mass flux through the specimen until steady-state diffusion is achieved. Experimental results using specimens of a geosynthetic clay liner subjected to potassium chloride solutions indicate that the measurement of ω may be affected by soil-solution interactions, as well as by changes in the induced chemico-osmotic pressure difference due to solute diffusion. As a result, ω should be evaluated using the induced pressure difference at steady state. The time required to achieve a steady-state response in induced pressure difference is related to the time required to achieve steady-state diffusion of all solutes, and may be affected by the circulation rate at the specimen boundaries. The circulation rate should be sufficiently rapid to minimize changes in the boundary concentrations due to diffusion, but sufficiently slow to allow measurement of solute mass flux at the lower concentration boundary for evaluating D^* and R_d.

KEYWORDS: chemico-osmosis, chemico-osmotic pressure, chemico-osmotic efficiency coefficient, coupled phenomena, diffusion testing, effective diffusion coefficient, geosynthetic clay liners, reflection coefficient, retardation factor

The ability of fine-grained (i.e., clay) soils to act as semipermeable membranes that inhibit the passage of electrolytes, and thereby cause chemico-osmotic flow, has been recognized as a possible cause of anomalous *in situ* pore-pressure measurements and groundwater movement (Marine and Fritz 1981, Olsen et al. 1990). The degree to which a clay soil inhibits the entry of ions into the pore space is termed chemico-osmotic efficiency and often is expressed quantitatively in terms of a chemico-osmotic efficiency coefficient, ω, or reflection coefficient, σ (e.g., see Staverman 1951, Kemper and Rollins 1966, Olsen et al. 1990, Keijzer et al. 1997). The theoretical chemico-osmotic efficiency coefficient of an "ideal" membrane that completely restricts the movement of electrolytes is unity (i.e., $\omega = 1$), whereas $\omega = 0$ for a material that exhibits no electrolyte restriction (e.g., Mitchell 1993). Clay soils that exhibit membrane behavior are considered "nonideal" membranes, since ω typically falls within the range $0 < \omega < 1$ (Kemper and Rollins 1966, Olsen 1969, Fritz and Marine 1983). The value of ω for a given clay soil is influenced by several factors, including the types and amounts of clay minerals in the soil, the sizes of pores, and the types and concentrations of electrolytes (Kemper and Rollins 1966, Bresler 1973, Olsen et al. 1990, Mitchell 1993).

The influence of chemico-osmotic efficiency on liquid migration in porous media typically is described using coupled flux theory based on the principles of irreversible thermodynamics applied to charged membranes (e.g., Katchalsky and Curran 1965, Olsen 1972, Yeung 1990, Mitchell 1993). At steady state, the horizontal, one-dimensional flux of an electrolyte solution through a charged membrane under isothermal conditions with no applied electrical gradient (i.e., $I = 0$) may be written as the sum of the Darcy flux, q_h, and a chemico-osmotic flux, q_π, as follows (Kemper and Rollins 1966, Barbour 1986):

$$q = q_h + q_\pi = -\frac{k_h}{\gamma_w}\frac{\Delta P}{\Delta x} + \omega\frac{k_h}{\gamma_w}\frac{\Delta \pi}{\Delta x} \tag{1}$$

where q is the total liquid flux, k_h is the hydraulic conductivity, γ_w is the unit weight of water, P is the liquid pressure, x is the direction of transport, and π is the chemico-osmotic pressure. The chemico-osmotic pressure difference, $\Delta\pi$, represents the theoretical pressure difference across an "ideal" semipermeable membrane (i.e., $\omega = 1$) that is required to prevent chemico-osmotic flux (e.g., see Olsen et al. 1990). Values of $\Delta\pi$ across a membrane separating ideal, dilute solutions can be computed using the van't Hoff expression (Barbour and Fredlund 1989), or

$$\Delta\pi = RT\sum_{i=1}^{N}\Delta C_i \tag{2}$$

where R is the universal gas constant [8.314 J $mol^{-1}{}^\circ K^{-1}$], T is the absolute temperature [$^\circ K$], ΔC_i represents the concentration difference of solute i across the membrane [$mol \cdot L^{-3}$], and N is the total number of solute species. The van't Hoff expression is based on the limiting assumption that the electrolyte solution is ideal and dilute and, therefore, provides only an approximate value of the chemico-

[1] Project engineer, GeoTrans, Inc., 9101 Harlan St. Suite 210, Westminster, CO 80030.

[2] Professor, Department of Civil Engineering, Colorado State University, Fort Collins, CO 80523, e-mail: shackel@engr.colostate.edu.

[3] Research professor, Division of Engineering, Colorado School of Mines, Golden, CO 80401.

* Corresponding author.

© 2001 by the American Society for Testing and Materials

osmotic pressure difference. However, Fritz (1986) notes that the error associated with the van't Hoff expression does not exceed 5% for 1:1 electrolytes (e.g., NaCl, KCl) at concentrations <1.0 M.

An evaluation of the potential effect of chemico-osmotic flux, q_π, on liquid and solute migration through low-k_h clay soils with $\omega > 0$ based on Eq 1 will require the measurement of the chemico-osmotic efficiency coefficient, ω. Such an evaluation may be important, for example, with respect to the design and performance of low-k_h clay soils commonly used for waste containment. Thus, the purpose of this paper is to describe a new testing apparatus to measure the chemico-osmotic efficiency of clay soils in the presence of electrolyte solutions.

Background

Values of ω for clay soils have been measured in the laboratory using different methods. For example, Kemper and Rollins (1966) measured ω for sodium bentonite pastes with respect to different salts by conducting a two-stage test in which the chemico-osmotic flux, q_π, and Darcy flux, q_h, were measured separately for a single test specimen. In the first stage, q_π was evaluated by placing a soil specimen into a testing cell located between two reservoirs containing solutions with different electrolyte concentrations (i.e., $\Delta\pi > 0$), but the same hydraulic pressure (i.e., $\Delta P = 0$). For these conditions, $q_h = 0$ such that, from Eq 1,

$$q|_{\Delta P=0} = q_\pi = \omega \frac{k_h}{\gamma_w} \frac{\Delta\pi}{\Delta x} \tag{3}$$

The chemico-osmotic flux, q_π, was measured by monitoring the change in height of the solutions in standpipes connected to the reservoirs.

In the second stage, q_h was evaluated by permeating the same soil specimen with a solution containing equal parts of the solutions used in the chemico-osmotic stage (i.e., the average solution) under a controlled hydraulic pressure difference (i.e., $-\Delta P > 0$). Since $\Delta\pi = 0$ at steady state under these conditions, $q_\pi = 0$ such that, from Eq 1,

$$q|_{\Delta\pi=0} = q_h = -\frac{k_h}{\gamma_w} \frac{\Delta P}{\Delta x} \tag{4}$$

The Darcy flux, q_h, was measured by monitoring liquid elevations in the standpipes. The expression used by Kemper and Rollins (1966) to calculate ω based on the results of the two testing stages is obtained by dividing Eq 4 by Eq 3, or

$$\omega = -\frac{q_\pi \Delta P}{q_h \Delta\pi} \tag{5}$$

The method proposed by Kemper and Rollins (1966) was used also by Letey et al. (1969) to measure ω of loams from natural deposits, and by Kemper and Quirk (1972) to measure ω of pure clays, including illite, kaolinite, and sodium bentonite.

Although the test procedure proposed by Kemper and Rollins (1966) is simple to assemble and perform, two separate testing stages must be conducted to obtain measured values of ω. Also, variations in the applied chemico-osmotic pressure difference, Δπ, will occur unless an attempt is made to maintain constant electrolyte concentrations at the specimen boundaries.

Olsen (1969) described a different approach for measuring ω. The apparatus used by Olsen (1969) to measure ω for saturated kaolinite specimens in the presence of NaCl solutions consisted of a confining cylinder with pistons to control the vertical stress on the specimen. The specimen was separated from the pistons with porous ceramic discs that transmit liquid between the clay and the piston channels (Olsen 1969). Solutions of different concentration of NaCl were introduced at the specimen boundaries through the piston channels, and flow through the specimen was superimposed using a syringe pump. Hydraulic head differences across the specimen were measured using a differential pressure transducer.

An example of the experimental results presented by Olsen (1969) is shown in Fig. 1 as a plot of head difference, Δ*H,* across the

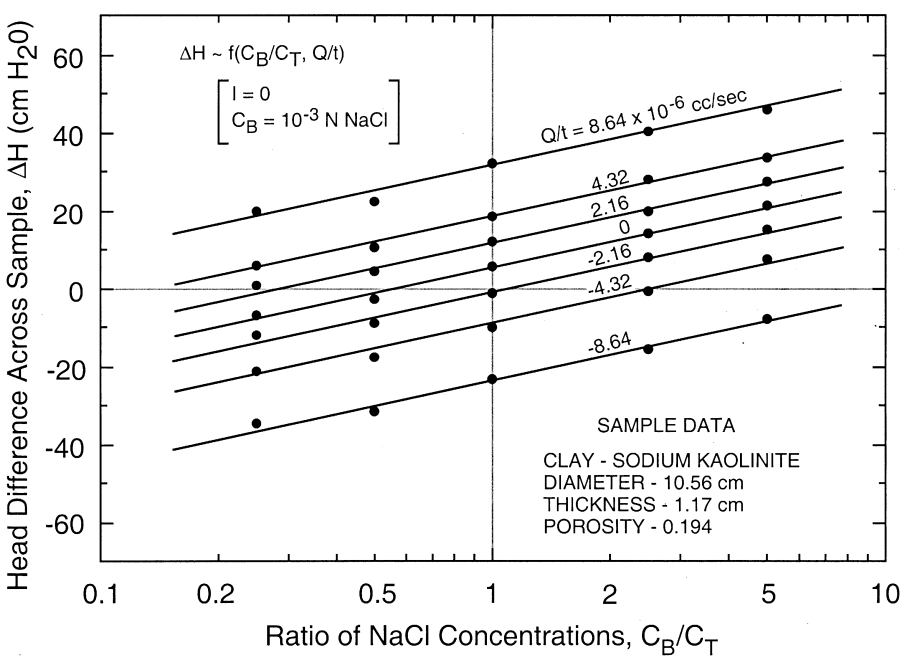

FIG. 1—*Measured head differences (*ΔH*) across a kaolinite specimen as a function of externally imposed flow rates (*Q/t*) and the ratio of NaCl concentrations at the specimen boundaries (*C_B/C_T*) (replotted after Olsen 1969).*

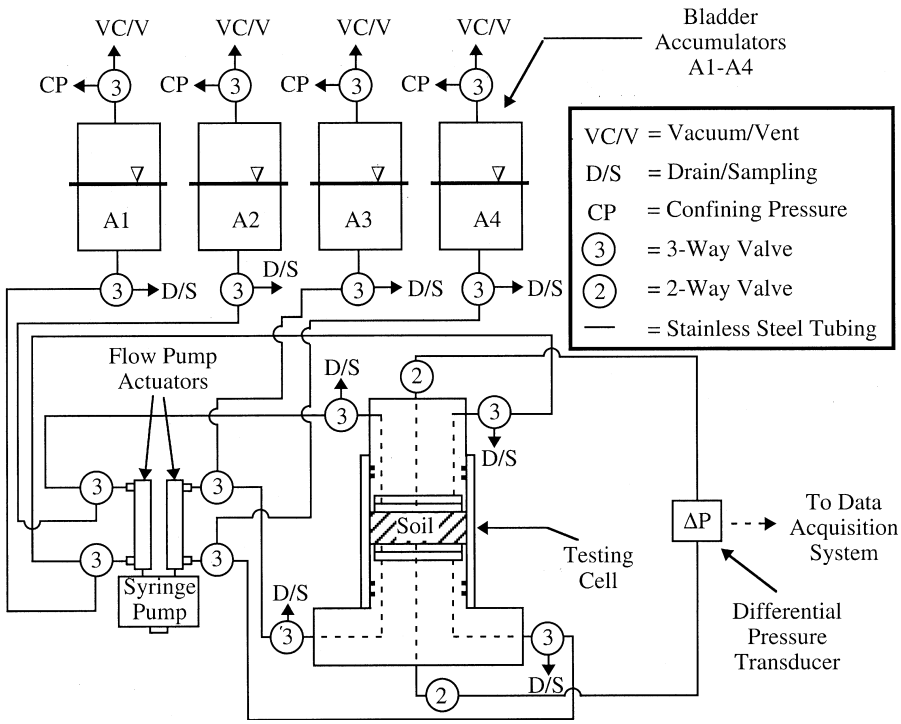

FIG. 2—*Schematic of chemico-osmotic testing apparatus used in this study.*

specimen versus the ratio of the solute concentrations at the bottom and top of the specimen, C_B/C_T. Separate curves are shown in Fig. 1 for each applied flow rate (designated as Q/t). The chemico-osmotic efficiency coefficient, ω, was determined using the results in Fig. 1 in accordance with the following relationship (Olsen 1969):

$$\omega = \frac{\Delta H/\log(C_B/C_T)}{RTC_B/\gamma_w} \tag{6}$$

where the numerator in Eq 6 represents the slope of the data shown in Fig. 1.

The method of Olsen (1969) represents a multistage approach to measure ω, since several different values of C_B/C_T must be applied to define the slopes shown in Fig. 1. Olsen (1969) indicated that the response time of the system was sufficiently rapid such that individual measurements were obtained within minutes after changing the boundary concentrations. As a result, measurement of ω using the approach of Olsen (1969) probably is more rapid than using the approach of Kemper and Rollins (1966). However, Olsen (1969) also noted that the system probably was not at a true steady state, since the testing durations were much shorter than the time that would be required for sufficient diffusion of the electrolyte to establish a steady-state concentration distribution within the soil specimen.

The advantages of the new testing apparatus and corresponding measurement approach described in this paper relative to the existing systems include the ability to (1) measure chemico-osmotic efficiency based on the results of a one-stage test, (2) maintain constant boundary electrolyte concentrations and, thus, a constant chemico-osmotic pressure difference, $\Delta\pi$, throughout the testing duration, and (3) measure simultaneously both ω, and the effective diffusion coefficient (D^*) and retardation factor (R_d) of the solutes. The results of laboratory tests on a geosynthetic clay liner (GCL) using potassium chloride (KCl) solutions are presented to illustrate these measurements.

New Testing Apparatus and Procedures

The chemico-osmotic testing apparatus proposed in this study is illustrated schematically in Fig. 2 and pictorially in Fig. 3. The primary components of the apparatus include a testing cell, a flow-pump system with two stainless steel actuators (syringes), stainless steel tubing to control the circulation of electrolyte solutions at the boundaries of the soil specimen, a differential pressure transducer, and bladder accumulators to collect the circulated solutions and refill the actuators. Additional details pertaining to these components follow.

Testing Cell

The chemico-osmotic testing cell consists of an acrylic cylinder (7.1-cm diameter), top piston, and base pedestal, as shown in Fig. 4. The design is similar to that used by Olsen (1969). The top piston is used to control the vertical stress or void ratio of the soil specimen and can be locked in place to prevent soil expansion. The top piston and base pedestal are equipped with ports that enable circulation of separate electrolyte solutions through porous stones at the specimen boundaries to establish and maintain a constant concentration difference across the specimen. Additional ports are installed in the top piston and base pedestal to allow for measurement of differential pressure across the specimen.

Flow-Pump System

The electrolyte solutions are circulated through the porous stones at the ends of the specimen using a flow-pump system consisting of a dual-carriage syringe pump (Model 944, Harvard Apparatus, South Natick, MA) equipped with two custom actuators to provide circulation of separate solutions through the top piston and base pedestal. A schematic of the flow-pump system is shown in Fig. 5. The Model 944 syringe pump is the same as that described

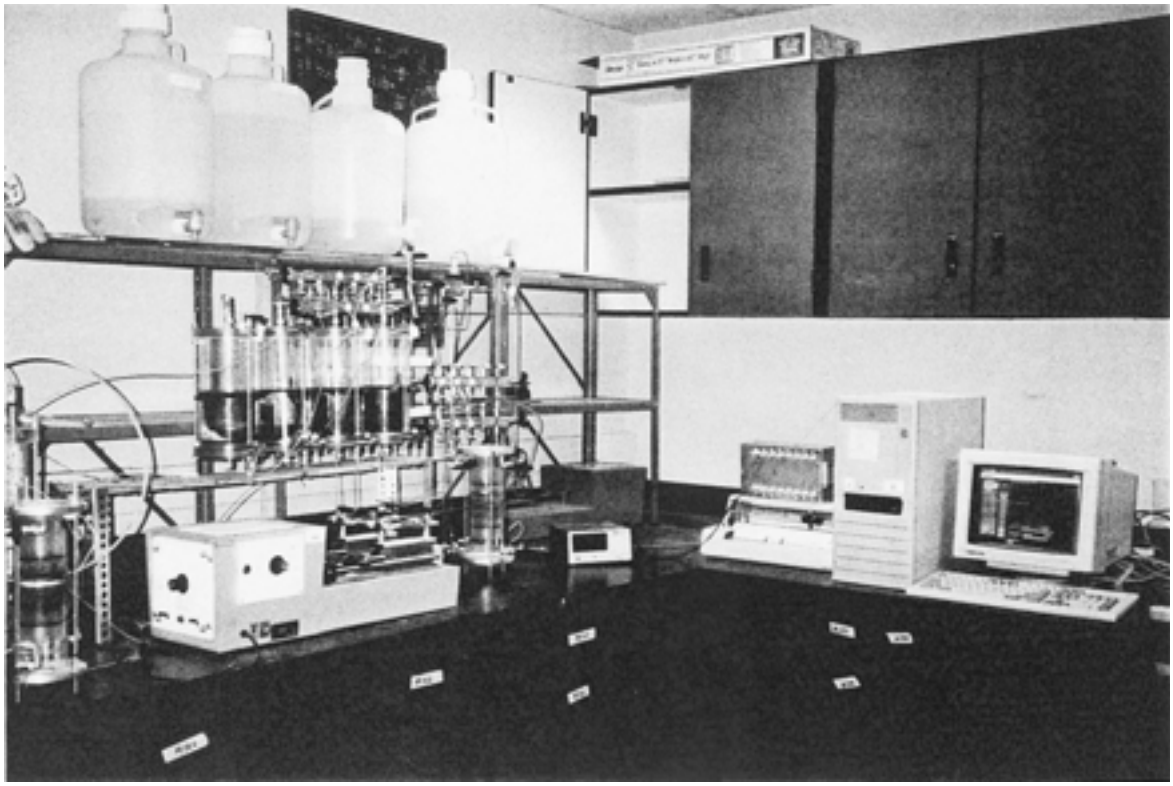

FIG. 3—*Pictorial view of chemico-osmotic testing apparatus used in this study.*

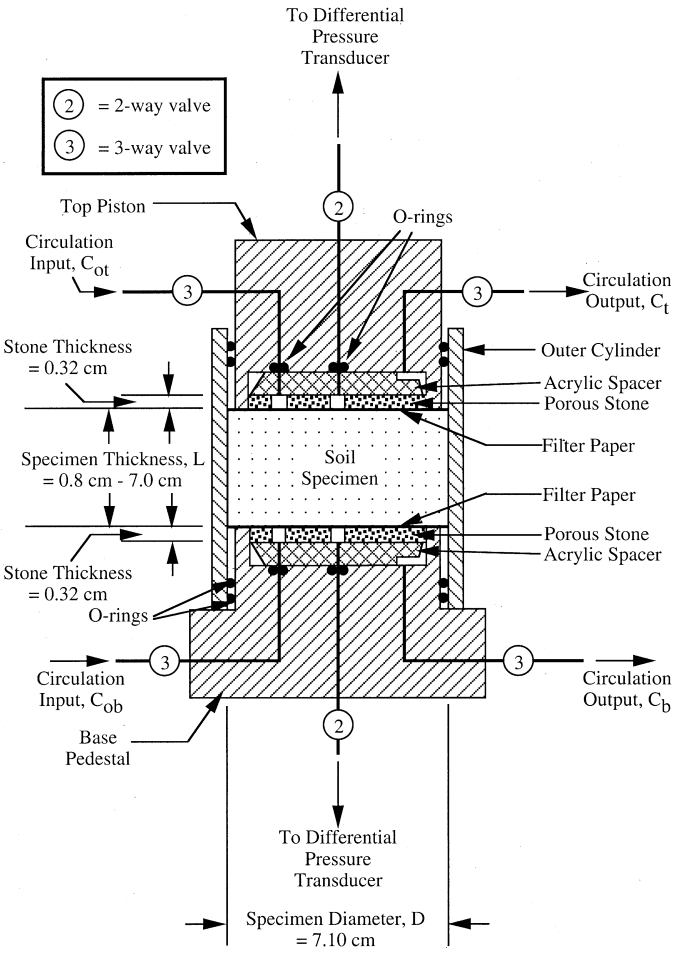

FIG. 4—*Schematic of chemico-osmotic testing cell.*

in Redmond and Shackelford (1994). The pump offers twelve gear selections and an additional variable speed control to provide linear displacement rates ranging from approximately 2.1×10^{-8} to 1.1×10^{-3} m/s. The two individual plungers are connected to lead screws from a single pump motor that drives the plungers at the same rate through the actuators, displacing liquid at the selected rate. The plungers can be operated in the same direction (i.e., parallel motion) or in opposite directions (i.e., reciprocal motion).

Flow-Pump Actuators

The actuators (syringes) mounted on the syringe pump consist of an outer housing with an inner bore that contains the plunger, as shown in Fig. 5*b*. Electrolyte solution contained within the annular area around the plunger shaft is forced from the actuator by the plunger barrel, which contains a groove for an O-ring to create a seal between the barrel and the inner wall of the housing. Liquid is forced from the actuators through ports installed in the end-caps that are attached to the ends of the housing with screws, as shown in Fig. 6*a*. All actuator parts were constructed with Grade 316 stainless steel to minimize corrosion in the presence of strong electrolytes.

The dimensions and manufacturing tolerances of the actuator housing, plunger shaft, and plunger barrel are shown in Fig. 6*b*. The dimensions of the actuator parts were selected based on the size of the Model 944 pump carriage and the range of flow rates desired in this study and, therefore, may not be appropriate for other flow-pump systems or other applications in which a different range of flow rates is required. For example, the measured flow rates for the actuators used in this study ranged from 9.2×10^{-12} to 4.7×10^{-7} m^3/s. A lower desired range of flow rates requires a smaller bore size in the actuator housing or a larger plunger shaft. However, the manufacturing tolerances (Fig. 6*b*) associated with the diameter of the bore, plunger shaft, and plunger barrel are recom-

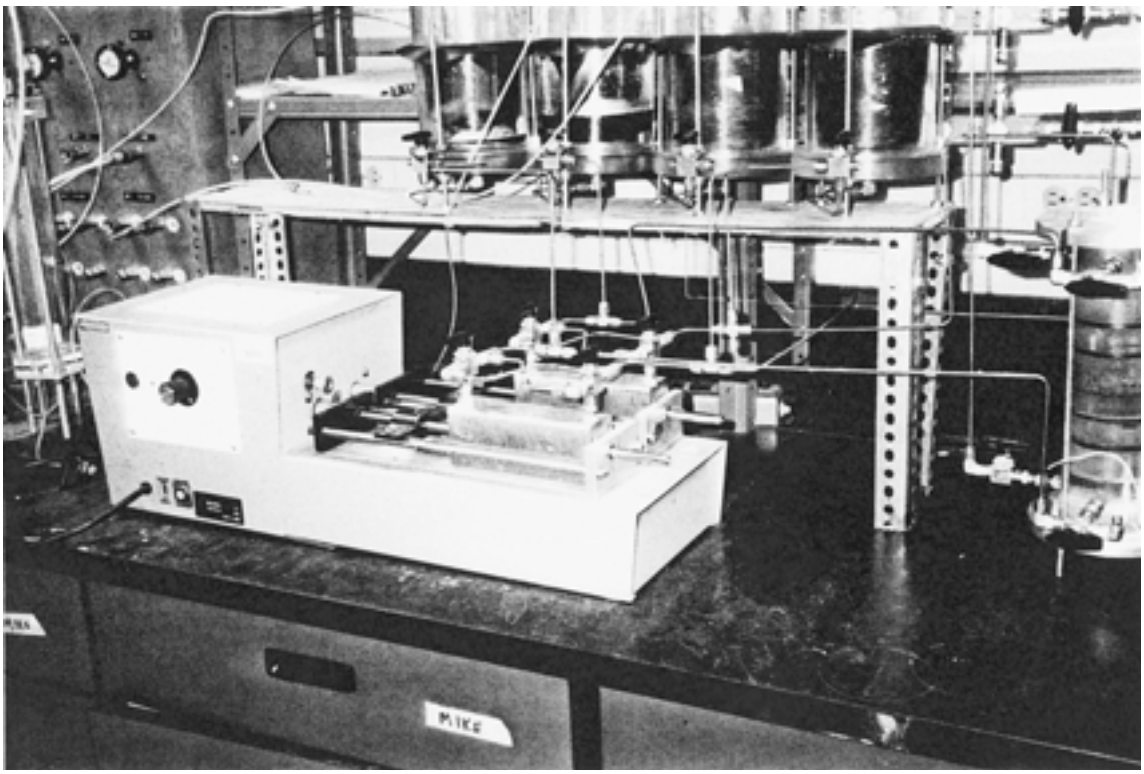

(a)

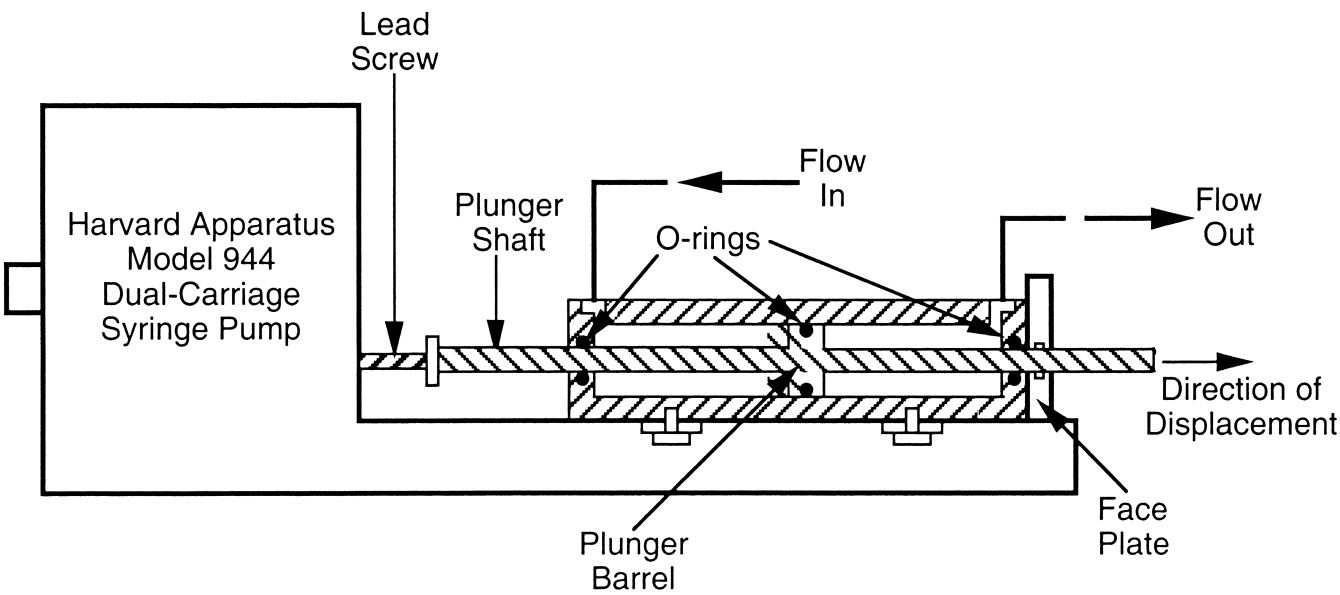

(b)

FIG. 5—*Illustrations of flow-pump system used in study:* (a) *pictorial view;* (b) *schematic cross section.*

mended for this actuator design, regardless of the dimensions, to ensure that a proper seal is maintained with the installed O-rings.

An advantage of this actuator design relative to other designs is the capability of infusing and withdrawing liquid at identical rates (see Olsen et al. 1991). For example, liquid can be expelled at one end of the housing and simultaneously collected at the same rate on the rear side of the plunger barrel through the port in the opposite end-cap. As a result of this capability, the two actuators are used in the chemico-osmotic test as individual circulation loops through the top piston and base pedestal to introduce fresh electrolyte solution continuously at the specimen boundaries, as shown in Fig. 7.

Once the plunger barrel reaches the end of the actuator housing, the actuator must be refilled with fresh electrolyte solution by reversing the pump direction and replenishing the actuator from an accumulator. The circulation outflow previously collected inside the actuator housing is purged simultaneously into a separate accumulator for subsequent chemical analysis (e.g., pH, electrical conductance, and solute concentrations). All tubing used to circulate

the solutions and refill the actuators is constructed with Grade 316 stainless steel to minimize corrosion and to prevent volume change in the system.

Measured solute concentrations in the purged solutions are used to evaluate the solute mass flux entering the soil from the higher concentration boundary and exiting the soil into the lower concentration boundary, due to diffusion. For example, if we assume in Fig. 7 that the solute concentration introduced into the top piston, C_{ot}, is greater than the solute concentration introduced into the base pedestal, C_{ob} (i.e., $C_{ot} > C_{ob}$), the difference in these concentrations represents a driving force for solute diffusion through the soil from the top piston to the base pedestal. As indicated in Fig. 7, the diffusive flux results in a lower concentration in circulation outflow from the top piston, C_t (i.e., $C_t < C_{ot}$), and a higher concentration in circulation outflow from the base pedestal, C_b (i.e., $C_b > C_{ob}$) as the solutions pass through the end-caps of the testing cell and back into the actuator housing. The measured concentrations, C_b and C_t, are used to compute the chemico-osmotic pressure difference across the specimen, $\Delta\pi$, and to evaluate the solute transport parameters (D^* and R_d).

Measurement of Chemico-Osmotic Efficiency

In order to measure the chemico-osmotic efficiency coefficient, the solutions are circulated through the specimen boundaries as shown in Fig. 7 to maintain a constant concentration difference across the specimen while maintaining a constant volume inside the testing cell (i.e., $\Delta V_{\text{cell}} = 0$). Since the volume of solution infused into either end of the testing cell is equal to the volume of solution withdrawn during circulation, no additional flux of solution can enter or exit the specimen boundaries. Therefore, solution flux through the soil cannot occur. This condition is represented mathematically by setting $q = 0$ in Eq 1, or

$$-\frac{k_h}{\gamma_w}\frac{\Delta P}{\Delta x} + \frac{\omega k_h}{\gamma_w}\frac{\Delta \pi}{\Delta x} = 0 \tag{7}$$

Rearrangement of Eq 7 yields the following expression for the chemico-osmotic efficiency coefficient, ω (Katchalsky and Curran 1965, Groenevelt and Elrick 1976, and van Oort et al. 1996):

$$\omega = \left.\frac{\Delta P}{\Delta \pi}\right|_{q=0} \tag{8}$$

The hydraulic pressure difference, ΔP, is induced across the specimen as a result of prohibiting the chemico-osmotic flux of solution that otherwise would occur in response to the applied concentration difference (e.g., see Keijzer et al. 1997). This induced pressure difference is measured with a differential pressure transducer (Model DP15, Validyne Engineering Sales Corp., Northridge, CA). The transducer is used in conjunction with a demodulator (Model CD223, Validyne Engineering Sales Corp., Northridge, CA) for conversion of the transducer signal into units of pressure. An analog output channel on the demodulator is used to transmit the pressure data continuously to a personal computer equipped with an OMEGA

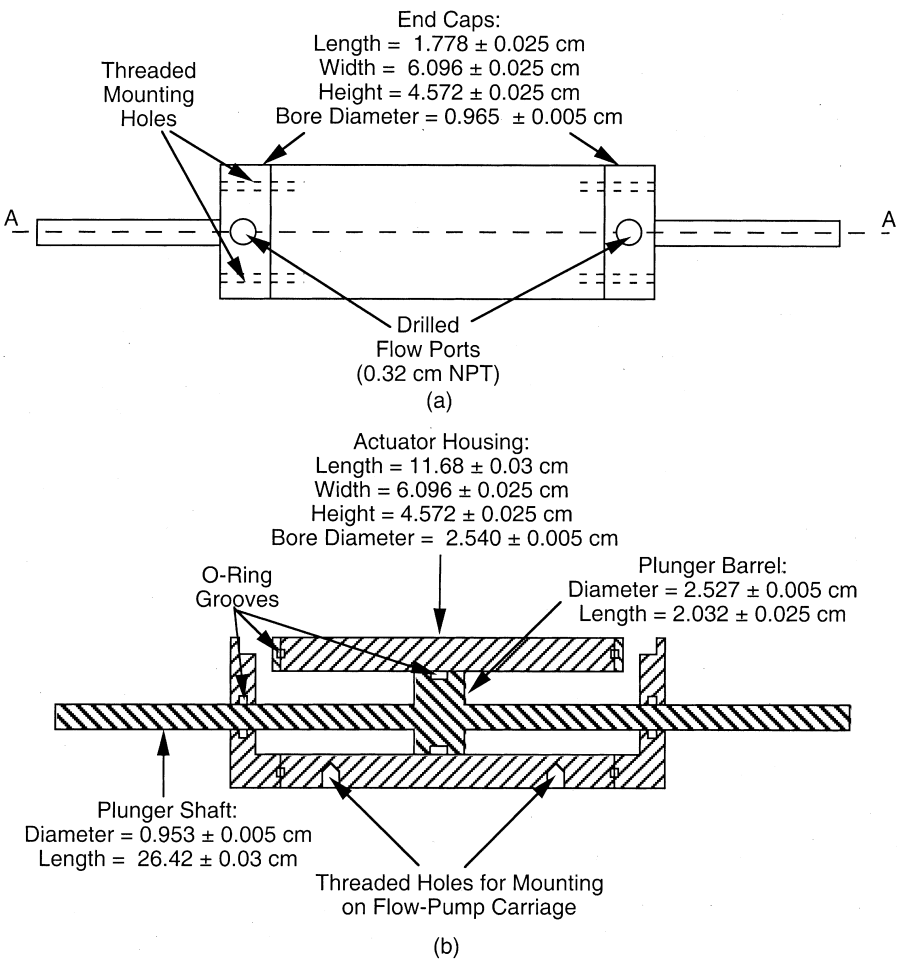

FIG. 6—*Schematics of flow-pump actuator: (*a*) top view; (*b*) cross-sectional view.*

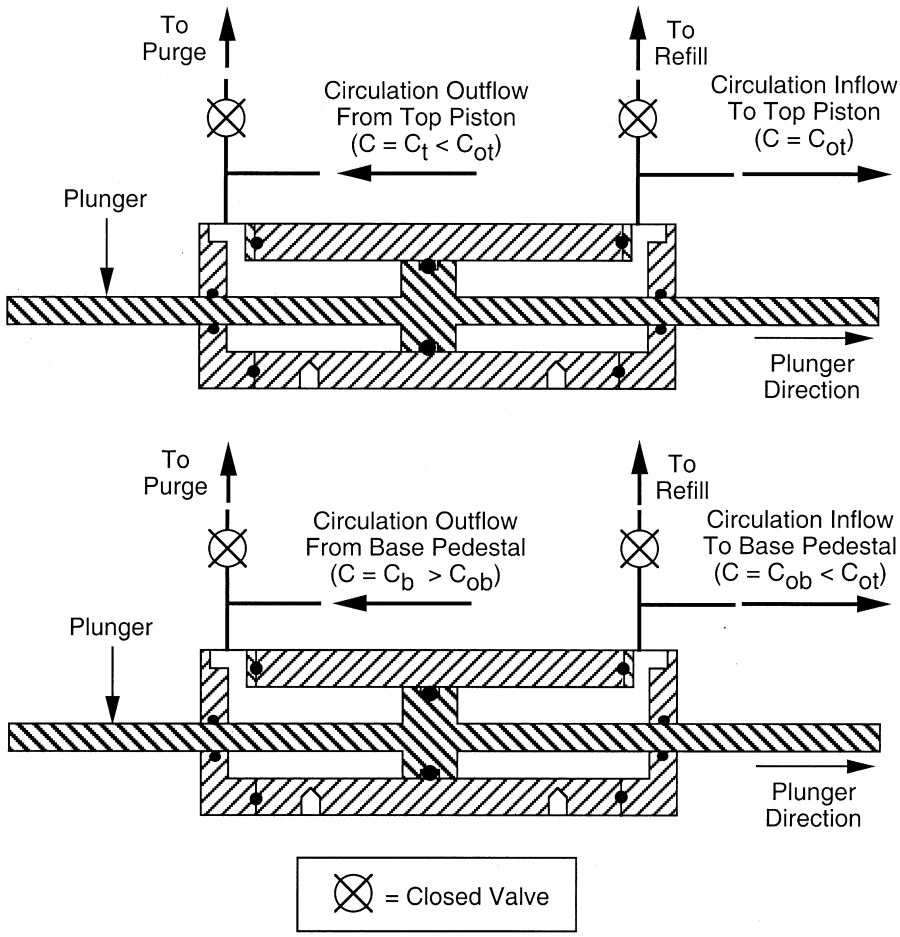

FIG. 7—*Schematic of top and bottom actuators during constant-volume circulation of electrolyte solutions at soil specimen boundaries.*

Model 100A DAQ board (OMEGA Engineering Inc., Stamford, CT) and the LabVIEW data acquisition software (National Instruments Corp., Austin, TX, Version IV), as illustrated in Fig. 8.

The chemico-osmotic pressure difference, $\Delta\pi$, in Eq 8 can be computed based on the solute concentrations in the opposite specimen boundaries in accordance with the van't Hoff expression (Eq 2). Since $C_t < C_{ot}$ and $C_b > C_{ob}$ due to solute diffusion (see Fig. 7), we may define the average boundary concentrations of a solute species *i*, $\overline{C}_{t,i}$ and $\overline{C}_{b,i}$, as follows:

$$\overline{C}_{t,i} = \frac{C_{ot,i} + C_{t,i}}{2} \tag{9a}$$

$$\overline{C}_{b,i} = \frac{C_{ob,i} + C_{b,i}}{2} \tag{9b}$$

Based on these average concentrations, the average chemico-osmotic pressure difference, $\overline{\Delta\pi}$, can be written as follows in accordance with Eq 2:

$$\overline{\Delta\pi} = RT\sum_{i=1}^{N}(\overline{C}_{b,i} - \overline{C}_{t,i}) \tag{10}$$

In accordance with Eq 10, $\overline{\Delta\pi} < 0$ when $\overline{C}_{t,i} > \overline{C}_{b,i}$.

Measurement of Transport Parameters

The effective diffusion coefficient, D^*, and retardation factor, R_d, for a solute species *i* is based on solute concentrations measured in the circulation outflow from the lower concentration boundary (i.e., the base pedestal) during the test in a similar manner to that previously described by Jessberger and Onnich (1994). This approach to measuring D^* and R_d is referred to commonly as the steady-state approach (Shackelford 1991).

In the steady-state approach, the measured concentrations for a given solute, C_b, typically are converted to cumulative mass per unit cross-sectional area, Q_t, or

$$Q_t = \frac{1}{A}\sum_{j=1}^{N_t}\Delta m_j = \frac{1}{A}\sum_{j=1}^{N_t}C_{b,j}\Delta V_j \tag{11}$$

where Δm is the incremental mass of the solute collected over a time increment (Δt), C_b is the concentration of the solute in the incremental volume, ΔV, of circulation outflow from the base pedestal corresponding to the same Δt, and N_t is the number of incremental samples *j* corresponding to the total elapsed time, *t*. The results are plotted in terms of Q_t versus *t*, as illustrated in Fig. 9. The curved portion of the example plot in Fig. 9 represents transient diffusion, while the linear portion of the data in Fig. 9 represents steady-state diffusion (Shackelford 1991). The analytical solution for Q_t at steady state based on one-dimensional diffusion with a constant source concentration, C_{ot}, in the top piston and a perfectly flushing boundary condition in the base pedestal (i.e., $C_{ob} = 0$) can be written as follows (Crank 1975, Shackelford 1991):

$$Q_t = \frac{nD^*C_{ot}}{L}t - \frac{nR_dLC_{ot}}{6} \tag{12}$$

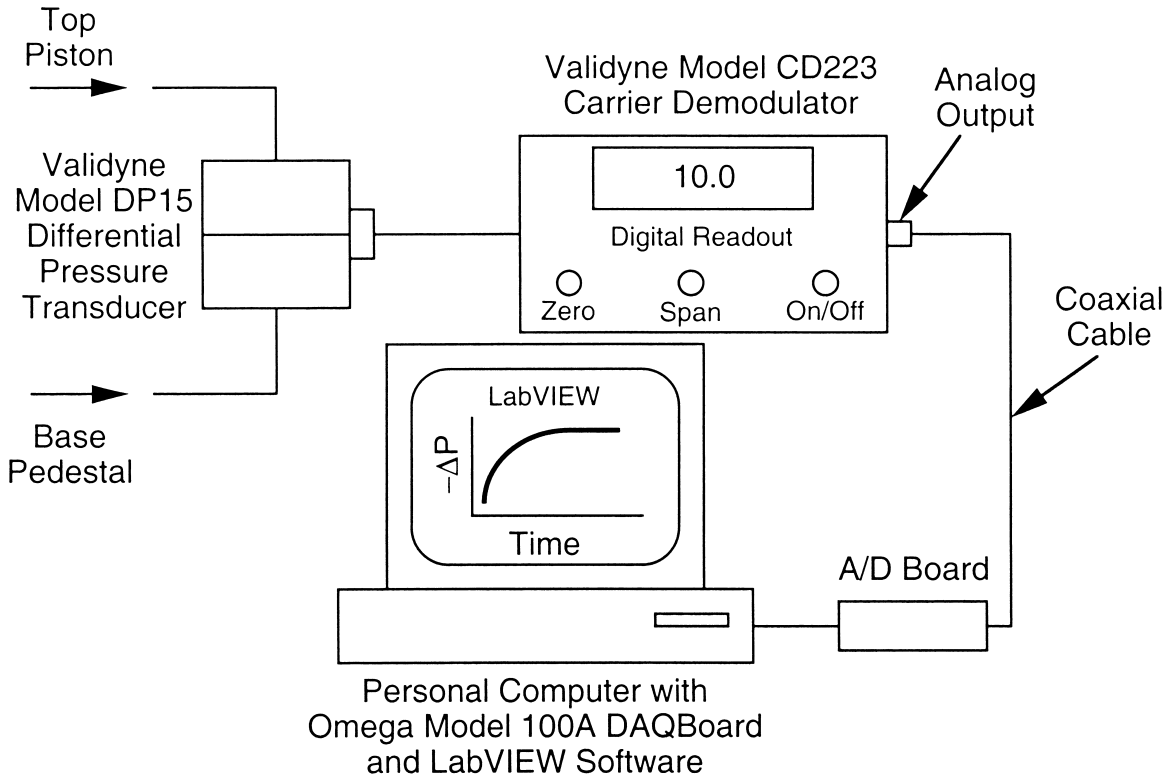

(a)

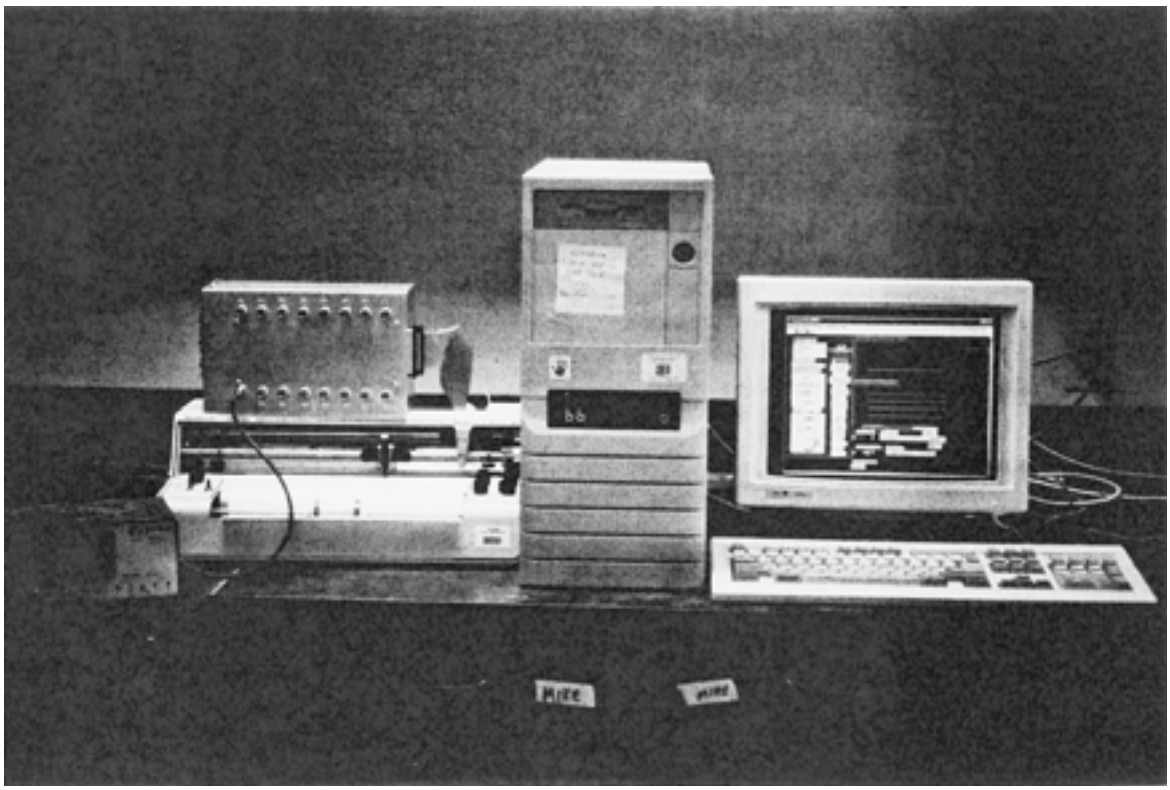

(b)

FIG. 8—*Differential pressure measurement and data acquisition system:* (a) *schematic view;* (b) *pictorial view.*

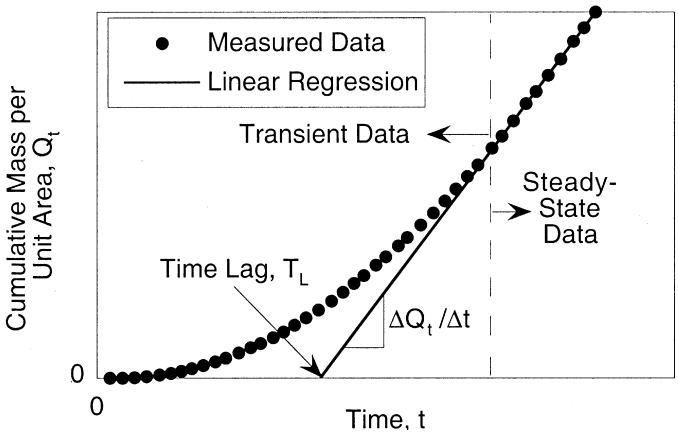

FIG. 9—*Schematic illustration of steady-state diffusion test results.*

where n is the specimen porosity, D^* is the effective diffusion coefficient, L is the specimen thickness, and R_d is the retardation factor. By inspection, Eq 12 represents a straight line through the steady-state data, as shown in Fig. 9. Typically, the slope, $\Delta Q_t/\Delta t$, in Fig. 9 is determined by best-fit linear regression of the steady-state data and used to compute the effective diffusion coefficient, D^*, of the given solute species in accordance with Eq 12, or

$$D^* = \left(\frac{\Delta Q_t}{\Delta t}\right)\left(\frac{L}{nC_{ot}}\right) \tag{13}$$

The retardation factor of the solute, R_d, is evaluated by determining the time tag, T_L, that represents the intercept of the regressed line through the steady-state data on the t-axis in Fig. 9. The intercept, T_L, is related to R_d by setting $Q_t = 0$ in Eq 12 and rearranging the resulting expression for R_d as follows (Shackelford 1991):

$$R_d = \frac{6D^*}{L^2}T_L \tag{14}$$

where D^* is determined previously from Eq 13.

Example Results

Some example results illustrating the performance of the testing apparatus are presented herein based on two tests conducted on separate 0.010-m-thick geosynthetic clay liner (GCL) specimens. A GCL was chosen for testing due to the presence of sodium bentonite, which is expected to exhibit measurable chemico-osmotic efficiency based on previous studies (e.g., Kemper and Rollins 1966). In addition, GCLs commonly are used either individually or as components of waste containment liners and cover systems (Daniel 1993, Koerner 1994). The GCL used in this study is sold commercially under the trade name Bentomat® (Colloid Environmental Technologies Company (CETCO), Lovell, WY). The Bentomat® GCL consists of a layer of granular sodium bentonite between two nonwoven polypropylene geotextiles held together by needle-punched fibers. Although the bentonite is regarded as a sodium bentonite, the results of the exchangeable cation measurements presented in Table 1 indicate that an appreciable amount of calcium (Ca^{2+}) is present also on the exchange sites of the bentonite. The procedures associated with measurement of the exchangeable cations shown in Table 1 are described in detail by Shackelford and Redmond (1995).

Circular GCL specimens were cut from a larger GCL sheet, placed in the testing cell, and permeated under back pressure with a processed tap water (PTW) to saturate the specimen, remove excess soluble salts, and measure hydraulic conductivity. The PTW was processed by passing tap water through three Barnstead® ion exchange columns in series, resulting in no measurable potassium or chloride, a measured pH of 6.93, and a measured electrical conductance (EC) of 0.32 mS/m at 25°C. At the beginning of each test, PTW was circulated at both boundaries of the specimens (i.e., $C_{ot} = C_{ob} = 0$) at a flow rate of 4.2×10^{-10} m^3/s for approximately 4.5 days to establish a steady baseline pressure difference. The chemico-osmotic tests then were initiated by circulating 0.0087 M KCl ($= C_{ot}$) in the top piston in Test 1 ($L = 0.010$ m, $n = 0.79$) and 0.047 M KCl ($= C_{ot}$) in Test 2 ($L = 0.010$ m, $n = 0.78$), while maintaining $C_{ob} = 0$ in the base pedestal for both tests.

Chemico-Osmotic Efficiency Coefficient

Although the actual pressure differences, ΔP, induced across the GCL specimens are less than zero due to sign convention, the measured induced pressure differences are plotted as positive values (i.e., $-\Delta P > 0$) versus time in Fig. 10. The baseline pressure difference, $-\Delta P_o$, during the first 4.5 days of PTW circulation at both specimen boundaries (i.e., $C_{ot} = C_{ob} = 0$) reached steady values of approximately 2.5 kPa and 4.0 kPa, respectively, in the two tests. Introduction of 0.0087 M KCl into the top piston in Test 1 after 4.5 days resulted in an immediate and rapid increase in the pressure difference as shown in Fig. 10*a*, which reached a steady value, $-\Delta P_{ss}$, of 22.2 kPa. Introduction of 0.047 M KCl into the top piston in Test 2 after 4.5 days resulted in a steady value, $-\Delta P_{ss}$, of 32.0 kPa, as shown in Fig. 10*b*.

The nonzero baseline pressure difference measured while $C_{ot} = C_{ob} = 0$ in the two tests is similar to that observed by Olsen (1969), as indicated in Fig. 1 (i.e., $\Delta H > 0$ for $C_B/C_T = 1$ and $Q/t = 0$), and discussed by Olsen (1985) and Olsen et al. (1985). Possible reasons for this nonzero baseline pressure difference include the existence of very small flow rates through the specimen that constitute small deviations from the $q = 0$ condition assumed in the test (e.g., due to slight differences in the dimensions of the actuators), and/or differences in the hydraulic properties of the porous stones at the opposite ends of the specimen. In either case, this nonzero baseline pressure difference should not be included when evaluating chemico-osmotic efficiency. Therefore, evaluation of ω at steady state is based on the corrected $-\Delta P$ (i.e., $-(\Delta P_{ss} - \Delta P_o)$ of 19.7 kPa in Test 1 and 28.0 kPa in Test 2 (see Fig. 10).

The concentrations of K^+ and Cl^- in circulation outflow from the top piston and base pedestal in the two tests are shown in Figs. 11 and 12, respectively. The results for Test 1 (i.e., $C_{ot} = 0.0087$ M KCl) in Fig. 11 show that the average concentrations in the top piston and base pedestal at steady state are $\overline{C}_{t,ss} = 295$ mg/L and $\overline{C}_{b,ss} = 10.5$ mg/L, respectively, for Cl^-, and $\overline{C}_{t,ss} = 326$ mg/L and $\overline{C}_{b,ss} = 11.0$ mg/L, respectively, for K^+. The results for Test 2 (i.e., $C_{ot} = 0.047$ M KCl) in Fig. 12 show that the average concentrations at

TABLE 1—*Exchangeable cation concentrations for bentonite in Bentomat® GCL.*

Exchangeable Cation	Concentration (meq/100 g Dry Soil)
K^+	0.8
Na^+	31.0
Ca^{2+}	20.8
Mg^{2+}	6.4

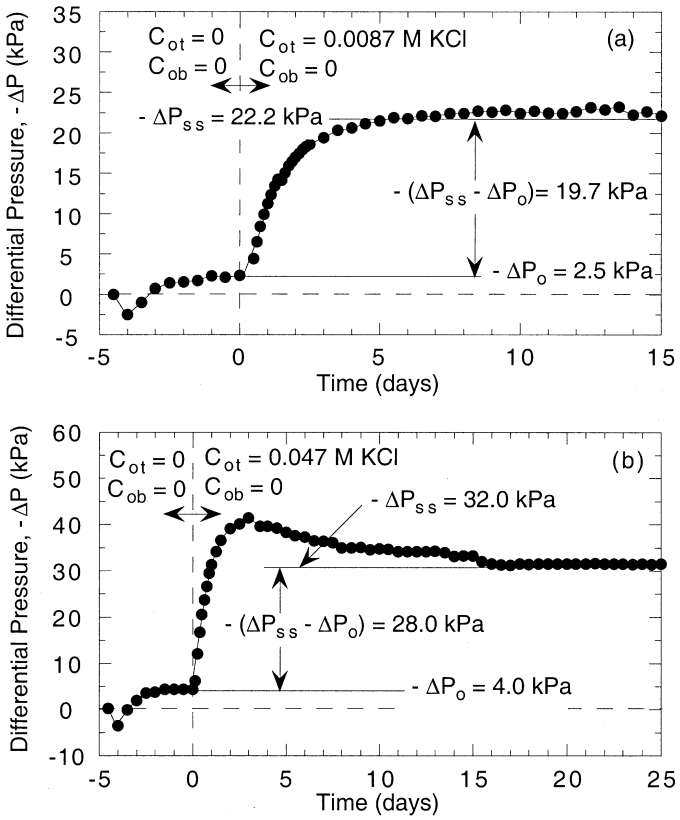

FIG. 10—*Pressure differences induced across 0.010-m thick GCL specimens: (*a*) Test 1; (*b*) Test 2.*

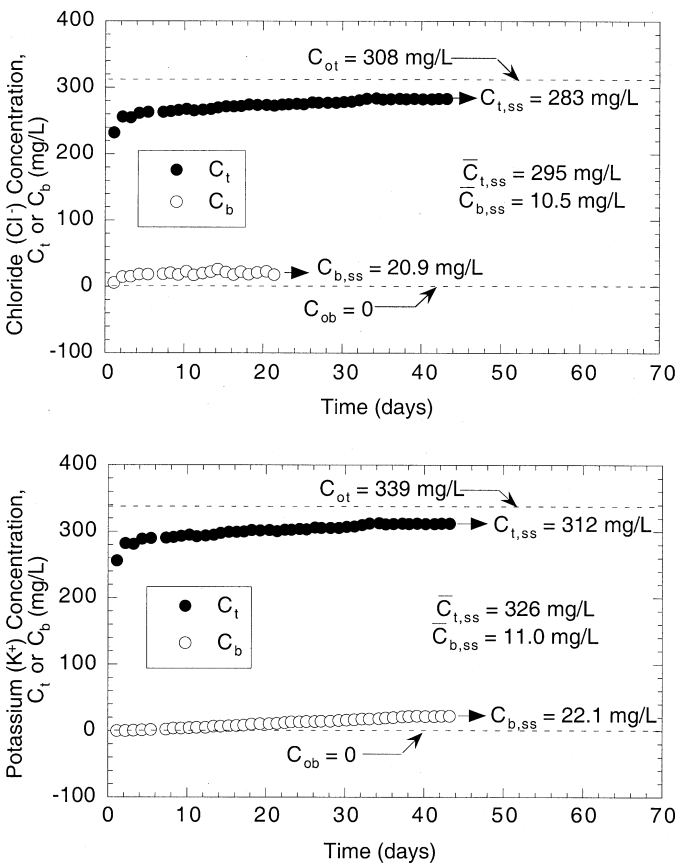

FIG. 11—*Boundary concentrations of chloride and potassium versus time for chemico-osmotic Test 1 (*C_{ot} *= 0.0087* M *KCl).*

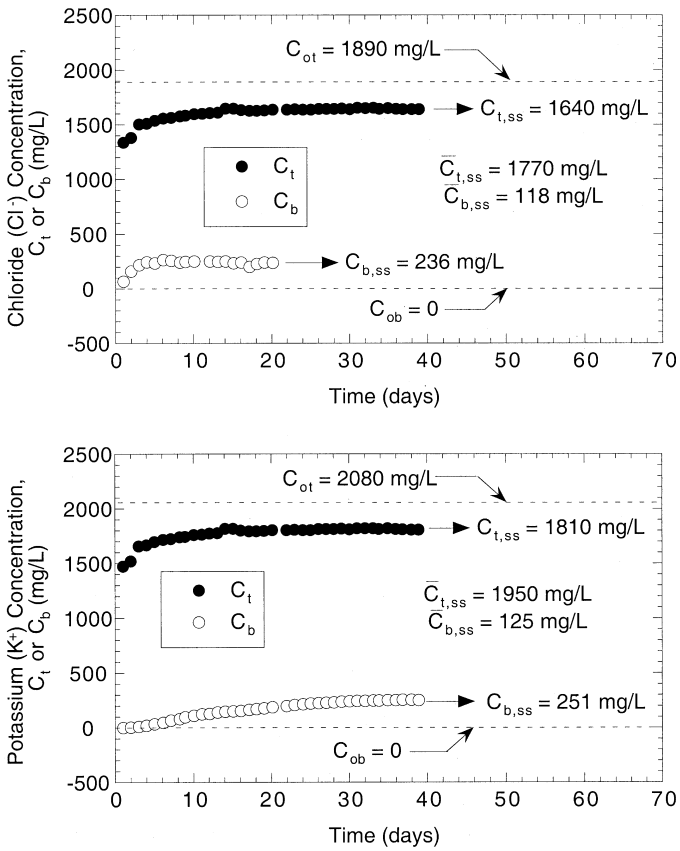

FIG. 12—*Boundary concentrations of chloride and potassium versus time for chemico-osmotic Test 2 (*C_{ot} *= 0.047* M *KCl).*

steady state in the top piston and base pedestal are $\overline{C}_{t,ss}$ = 1770 mg/L and $\overline{C}_{b,ss}$ = 118 mg/L, respectively, for Cl^-, and $\overline{C}_{t,ss}$ = 1950 mg/L and $\overline{C}_{b,ss}$ = 125 mg/L, respectively, for K^+. Based on these average concentrations, values of $-\Delta\pi$ across the specimens at steady state are 39.9 kPa in Test 1 and 201 kPa in Test 2 (see Eq 10). The resulting values of ω at steady state are 0.49 (i.e., 19.7 kPa/39.9 kPa) in Test 1 and 0.14 (i.e., 28.0 kPa/201 kPa) in Test 2. These results are consistent with previous results for bentonite in that ω decreases with increasing average solute concentration across the soil (e.g., Kemper and Rollins 1966).

The time required to achieve a steady induced pressure difference response is approximately six days in Test 1 (Fig. 10*a*) and 16 days in Test 2 (Fig. 10*b*). This time also corresponds essentially to the time required to achieve steady electrical conductance (EC) in the base pedestal in the two tests, as shown in Fig. 13. The steady EC indicates a steady concentration of total ions (i.e., anions plus cations) diffusing into the base pedestal. The correlation between the steady induced pressure difference and the steady EC is expected since the chemico-osmotic pressure difference, $\Delta\pi$, that controls the induced pressure difference for a given ω (i.e., $\Delta P = \omega \cdot \Delta\pi$), is a function of the difference in total solute concentration across the specimen in accordance with the van't Hoff expression (Eq 2).

Diffusion of the nonreactive species (i.e., Cl^-) represents the contribution of anions to the measured EC values in the base pedestal shown in Fig. 13. However, during the transient stage of the test, diffusion of the reactive species (i.e., K^+) represents only a portion of the total cation contribution to the EC values in the base pedestal. For example, the results in Figs. 11 and 12 show that

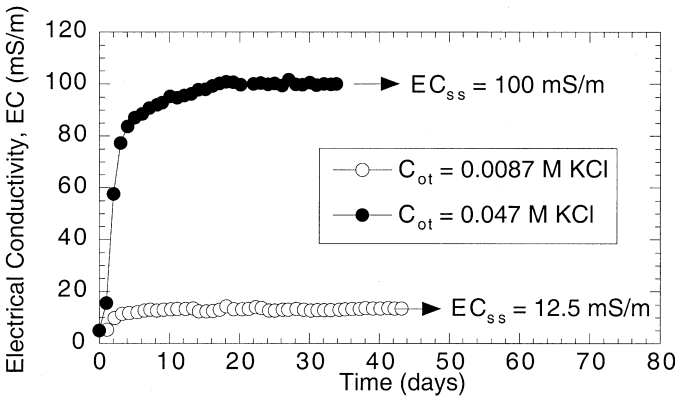

FIG. 13—*Measured electrical conductance in circulation outflow from base pedestal versus time in chemico-osmotic Tests 1 and 2.*

steady K^+ concentrations in the base pedestal are observed much later than steady Cl^- concentrations. Under the assumption that this delayed transport of K^+ is due to ion exchange, the adsorption of K^+ to the bentonite during this transient stage must be accompanied by desorption of the same number of equivalents of exchangeable cations in order to maintain electroneutrality in solution (Shackelford et al. 1999). As previously noted in Table 1, the dominant exchangeable cations associated with the bentonite of the GCL used in this study are Na^+ and Ca^{2+}. Although K^+ is more likely to exchange with Na^+ relative to Ca^{2+} on the basis of charge (Mitchell 1993), the desorption of either Na^+ or Ca^{2+} should result in a similar contribution to the overall EC in the base pedestal since the equivalent ionic conductances of Na^+ and Ca^{2+} are similar (Shackelford et al. 1999).

*Effective Diffusion Coefficient, D**

The results of the steady-state method to determine the effective diffusion coefficient, D^*, and the retardation factor, R_d, for Test 1 (i.e., C_{ot} = 0.0087 M KCl) are shown in Fig. 14. Steady-state diffusion into the base pedestal was observed after 144 h (6 days) for Cl^- and after 912 h (38 days) for K^+, based on the concentrations shown in Fig. 11. The slopes, $\Delta Q_t/\Delta t$, obtained from linear regression of the steady-state data are 2.82×10^{-6} g/m^2/s for Cl^- and 2.43×10^{-6} g/m^2/s for K^+. The resulting D^* values for Cl^- and K^+ are 1.16×10^{-10} m^2/s and 0.907×10^{-10} m^2/s, respectively. The closeness in the D^* values for Cl^- and K^+ is consistent with the requirement that these D^* values must be the same at steady-state diffusion due to electroneutrality (Shackelford and Daniel 1991). In addition, these values of D^* are similar to the steady-state salt (KCl) D^* values reported by Jessberger and Onnich (1994) for sand, gravel, and bentonite mixtures containing 14.4 percent sodium bentonite. For example, Jessberger and Onnich (1994) reported salt D^* values for 0.05 *M* KCl and 0.2 *M* KCl of 1.23×10^{-10} m^2/s and 1.34×10^{-10} m^2/s, respectively. However, the measured D^* values in this study do not account for the coupling effect that results from the salt sieving associated with clay membrane behavior (e.g., Groenevelt et al. 1980).

Retardation Factor, R_d

The T_L values for Test 1 based on linear regression of the data for Cl^- and K^+ in Fig. 14 are 56.6 h and 466 h, respectively. Thus, from Eq 12 with L = 0.010 m, n = 0.79, and the previously reported D^* values, the measured values of R_d are 1.4 for Cl^- and 9.1 for K^+. Values of R_d for nonreactive (i.e., nonadsorbing) solutes, typically anions such as chloride (Cl^-), are expected to be unity (i.e., R_d = 1) (e.g., Shackelford 1993). Therefore, the measured value of R_d for Cl^- is close to that expected for Cl^-. Conversely, the measured value of R_d for K^+ is consistent with the behavior of a reactive (i.e., adsorbed) solute in which $R_d > 1$. As noted earlier, the adsorption of K^+ in this test likely is due to ion exchange with Na^+ and/or Ca^{2+} at the clay particle surfaces.

Discussion

Soil-Solution Interaction

Membrane behavior in a clay soil is characterized by the restriction of ions from the soil pores. This restriction is caused by electric fields associated with the adsorbed ion layers (i.e., diffuse double layers) surrounding adjacent clay particles that extend into the pore space (Marine and Fritz 1981). The degree of ion restriction and, thus, the chemico-osmotic efficiency of the soil is governed by the thicknesses of these adsorbed layers. For example, the degree of ion restriction is greatest (i.e., ω = 1) when the adsorbed layers of adjacent particles completely overlap in the pore space, leaving no "free" space for solute transport.

The thickness of the adsorbed ion layer is influenced by pore fluid chemistry factors such as ion concentration, valence, dielectric constant, and temperature (Mitchell 1993). For example, an increase in ion concentration in the pore water causes a decrease in adsorbed layer thickness (Mitchell 1993). Therefore, an increase in solute concentration in the pore water of a soil during a chemico-

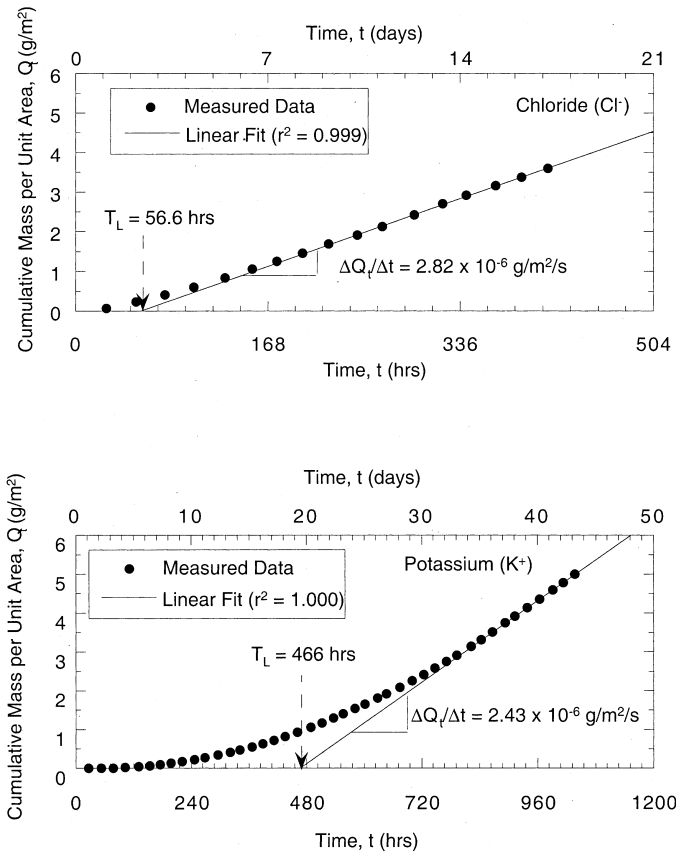

FIG. 14—*Results of steady-state method to evaluate the effective diffusion coefficient (D*) and retardation factor (R_d) in chemico-osmotic Test 1 for chloride and potassium (C_{ot} = 0.0087 M KCl, L = 0.010 m, n = 0.79).*

osmotic test due to solute diffusion could result in a time-dependent decrease in the chemico-osmotic efficiency.

In this study, the measured pressure differences, $-\Delta P$ (>0), shown in Fig. 10*b* for chemico-osmotic Test 2 (i.e., $C_{ot} = 0.047$ *M* KCl), increase to 40 kPa after approximately three days, but subsequently decrease before reaching a steady value of 32 kPa. The decrease in $-\Delta P$ in this test may be due to a time-dependent decrease in chemico-osmotic efficiency of the specimen as the KCl diffuses from the top piston into the base pedestal. Conversely, a time-dependent decrease in $-\Delta P$ was not observed in Test 1 (see Fig. 10*a*), probably because the solute concentration (i.e., 0.0087 *M* KCl) was not sufficiently high to cause a significant change in adsorbed layer thickness.

The potential for a time-dependent change in chemico-osmotic efficiency may be reflected indirectly through a change in hydraulic conductivity since an increase in electrolyte concentration also may result in an increase in hydraulic conductivity for relatively highly reactive clay soils, such as the sodium bentonites commonly used in GCLs (Shackelford et al. 2000). Therefore, the hydraulic conductivity of each GCL specimen was measured both before and after chemico-osmotic testing for comparison.

The results of these hydraulic conductivity measurements are shown in Fig. 15 for specimens subjected to $C_{ot} = 0.0087$ *M* KCl (Test 1) and $C_{ot} = 0.047$ *M* KCl (Test 2) during the chemico-osmotic tests. The results show that the hydraulic conductivity of the specimen subjected to 0.0087 *M* KCl during the chemico-osmotic test increased 36% from ~ 1.1×10^{-11} m/s before testing to ~ 1.5×10^{-11} m/s after testing. However, the hydraulic conductivity of the GCL specimen subjected to 0.047 *M* KCl during the chemico-osmotic test increased 61% from ~ 9.1×10^{-12} m/s before testing to ~ 1.5×10^{-11} m/s after testing. The slightly greater increase in k_h for the specimen subjected to the higher concentration of 0.047 *M* KCl is consistent with a greater decrease in adsorbed layer thickness during the chemico-osmotic test that also is likely responsible for the time-dependent decrease in $-\Delta P$ in Fig. 10*b*.

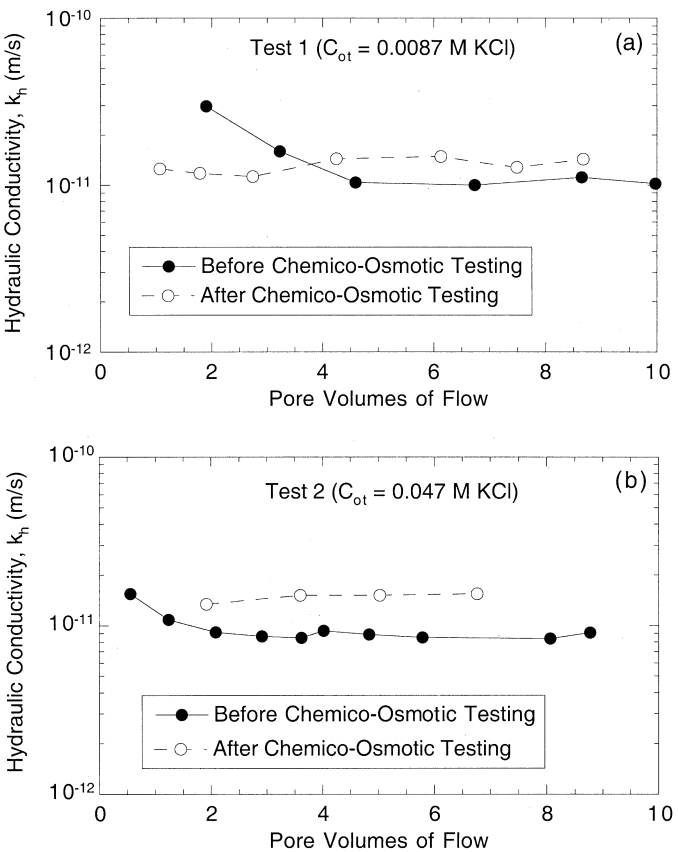

FIG. 15—*Hydraulic conductivity of GCL specimens before and after chemico-osmotic tests: (*a) $C_{ot} = 0.0087$ M *KCl; and (*b) $C_{ot} = 0.047$ M *KCl.*

Circulation Rate

At $t = 0$ in a chemico-osmotic test, the initial difference in chemico-osmotic pressure, $\Delta\pi_o$, computed in accordance with Eq 2 based on the initial concentrations, C_{ot} and C_{ob}, of all solutes in the circulated solutions, or

$$\Delta\pi_o = RT\sum_{i=1}^{N}(C_{ob,i} - C_{ot,i}) \tag{15}$$

represents the maximum possible (absolute) value of $\Delta\pi$ that can be maintained across the specimen. At $t > 0$, the value of $\Delta\pi$ and, thus, the induced ΔP are related to the rate of diffusion relative to the circulation rate of the electrolyte solutions at the specimen boundaries. For example, "perfectly flushing" boundary conditions are applied by imposing a sufficiently rapid circulation rate such that the changes in solute concentration at the specimen boundaries due to diffusion are negligible. In this case, $\overline{C}_t = C_{ot}$, $\overline{C}_b = C_{ob}$ and, therefore, $\overline{\Delta\pi} = \Delta\pi_o$ throughout the test. Conversely, if no attempt is made to maintain the boundary concentrations, diffusion will result in a decrease in solute mass in the top piston and an increase in solute mass in the base pedestal until $\overline{C}_t = \overline{C}_b$ and $\Delta\pi = 0$ at steady state. Likewise, any induced pressure difference, $-\Delta P$, that is generated during the transient stage of the test also will dissipate to zero at steady state (e.g., see Keijzer et al. 1997).

In this study, the circulation rate at the specimen boundaries was 4.2×10^{-10} m^3/s in both Test 1 and Test 2. This circulation rate was not sufficient to mimic "perfectly flushing" boundary conditions in either test, since $\overline{C}_t < C_{ot}$ and $\overline{C}_b > C_{ob}$ at steady state in both cases (see Figs. 11 and 12). However, the transient reduction in $\Delta\pi$ over time is greater in Test 1 than in Test 2. For example, values of $-\Delta\pi_o$ in Test 1 ($C_{ot} = 0.0087$ *M* KCl and $C_{ob} = 0$) and Test 2 ($C_{ot} = 0.047$ *M* KCl and $C_{ob} = 0$) are 43.0 kPa and 234 kPa, respectively. Therefore, at steady state, $-\overline{\Delta\pi}$ in Test 1 (39.9 kPa) is 7.2% lower than $-\Delta\pi_o$, whereas $-\overline{\Delta\pi}$ (201 kPa) is 14% lower than $-\Delta\pi_o$ in Test 2. The greater influence of diffusion on $-\overline{\Delta\pi}$ in Test 2 is due to the higher concentration gradient and resulting greater diffusive mass flux relative to Test 1. The greater reduction in $-\overline{\Delta\pi}$ in Test 2 may be responsible, in part, for the increase and subsequent decrease in the transient differential pressure response (Fig. 10*b*), and the corresponding longer time required to achieve a steady $-\Delta P$ (16 days) relative to Test 1 (6 days).

Use of the initial chemico-osmotic pressure difference, $\Delta\pi_o$, rather than the average chemico-osmotic pressure difference, $\overline{\Delta\pi}$, to evaluate ω is more convenient, since values of $\Delta\pi_o$ are computed easily based on the initial boundary solute concentrations (Eq 15). Therefore, evaluation of ω based on $\Delta\pi_o$ eliminates the need to measure solute concentrations, C_b and C_t, in the circulation outflow from the base pedestal. For example, in this study, the values of ω based on $\Delta\pi_o$ rather than $\overline{\Delta\pi}$ are 0.46 (i.e., 19.7 kPa/43.0 kPa) in Test 1 and 0.12 (i.e., 28.0 kPa/234 kPa) in Test 2. These values of ω are only slightly lower than the values of ω based on $\overline{\Delta\pi}$ (0.49 and 0.14, respectively). Nonetheless, the differences in these ω values represent the error associated with ignoring the influence of solute diffusion. This error can be reduced further by increasing the

circulation rate to reduce changes in the boundary solute concentrations. A faster circulation rate also could reduce the time required to achieve steady-state conditions. However, a circulation rate that is too rapid will dilute the concentrations of solutes diffusing from the specimen such that the ability to measure the solute mass flux into the base pedestal required for determination of D^* and R_d may be prohibited. Therefore, the optimal circulation rate should be sufficiently rapid to minimize changes in the boundary solute concentrations due to diffusion and to allow ω to be determined more conveniently based on $\Delta\pi_o$, but sufficiently slow to allow a measurable accumulation of solute mass into the base pedestal for determining D^* and R_d.

Summary and Conclusions

The design and performance of a testing apparatus to measure chemico-osmotic efficiency coefficients, ω, for clay soils in the presence of electrolytes is described. The testing cell that contains the soil specimen consists of a rigid cylinder, top piston, and base pedestal. The top piston and base pedestal are equipped with ports for measuring pressure differences across the specimen and for continuous circulation of different electrolyte solutions at the specimen boundaries. Electrolyte circulation is provided under constant-volume conditions using a dual-carriage flow-pump system with custom actuators (syringes) that facilitate infusion and withdrawal of the solutions across opposite specimen boundaries at identical rates, while preventing solution flux through the soil specimen. Thus, pressure differences are induced across the soil specimen due to the prevention of chemico-osmotic flux of solution through the soil that otherwise would occur as a result of the controlled difference in electrolyte concentration. This concentration difference represents a difference in chemico-osmotic pressure across the specimen that can be estimated using the van't Hoff expression. The chemico-osmotic efficiency coefficient, ω, represents the ratio of the induced pressure difference, ΔP, relative to the chemico-osmotic pressure difference, $\Delta\pi$.

The concentration difference applied by circulating the different electrolyte solutions at the specimen boundaries also represents a driving force for diffusion from the higher concentration boundary to the lower concentration boundary. Measured electrolyte concentrations in the circulation outflow from the lower concentration boundary can be used to determine the effective diffusion coefficient, D^*, and the retardation factor, R_d, for the solutes based on the steady-state approach.

The results of chemico-osmotic tests conducted on geosynthetic clay liner (GCL) specimens in the presence of KCl solutions indicate that the differential pressure response may be influenced by (1) time-dependent changes in chemico-osmotic efficiency due to soil-solution interactions, and (2) the circulation rate of the electrolyte solutions at the specimen boundaries relative to the rate of solute diffusion through the soil. The induced pressure difference is related directly to the difference in chemico-osmotic pressure, $\Delta\pi$, that is a function of the difference in electrolyte concentrations circulated at the opposite specimen boundaries. Solute diffusion through the soil results in a decrease in electrolyte concentration at the higher concentration boundary and an increase in electrolyte concentration at the lower concentration boundary. The overall effect is a net decrease in $\Delta\pi$, that likely is responsible, in part, for the initial increase and subsequent decrease in the induced pressure difference across a GCL specimen subjected to 0.047 *M* KCl. In general, changes in the boundary concentrations and, therefore, $\Delta\pi$, due to diffusion can be reduced or eliminated by increasing the circulation rate. A faster circulation rate also may reduce the time required to achieve steady-state conditions. However, the circulation rate should be sufficiently slow to allow measurement of solute mass flux at the lower concentration boundary for evaluating the solute transport parameters (D^* and R_d).

Acknowledgments

Financial support for this study, which was part of a collaborative research effort between Colorado State University (CSU) and the Colorado School of Mines (CSM), was provided by the U.S. National Science Foundation (NSF), Arlington, VA, under Grant CMS-9634649 for CSU and Grant CMS-9616855 for CSM. The opinions expressed in this paper are solely those of the writers and are not necessarily consistent with the policies or opinions of the NSF.

References

Barbour, S. L., 1986, *Osmotic Flow and Volume Change in Clay Soils,* Ph.D. Dissertation, University of Saskatchewan, Saskatoon.

Barbour, S. L. and Fredlund, D. G., 1989, "Mechanisms of Osmotic Flow and Volume Change in Clay Soils," *Canadian Geotechnical Journal,* Vol. 26, pp. 551–562.

Bresler, E., 1973, "Simultaneous Transport of Solutes and Water Under Transient Unsaturated Flow Conditions," *Water Resources Research,* Vol. 9, No. 4, pp. 975–986.

Crank, J., 1975, *The Mathematics of Diffusion,* 2nd ed., Clarendon Press, Oxford.

Daniel, D. E., 1993, "Clay Liners," Chap. 7, *Geotechnical Practice for Waste Disposal,* D. E. Daniel, Ed., Chapman and Hall, New York, pp. 137–163.

Fritz, S. J., 1986, "Ideality of Clay Membranes in Osmotic Processes: A Review," *Clays and Clay Minerals,* Vol. 34, No. 2, pp. 214–223.

Fritz, S. J. and Marine, I. W., 1983, "Experimental Support for a Predictive Osmotic Model of Clay Membranes," *Geochimica et Cosmochimica Acta,* Vol. 47, pp. 1515–1522.

Groenevelt, P. H. and Elrick, D. E., 1976, "Coupling Phenomena in Saturated Homo-ionic Montmorillonite: II. Theoretical," *Soil Science Society of America, Journal,* Vol. 40, pp. 820–823.

Groenevelt, P. H., Elrick, D. E., and Laryea, K. B., 1980, "Coupling Phenomena in Saturated Homoionic Montmorillonite: IV. The Dispersion Coefficient," *Soil Science Society of America, Journal,* Vol. 44, No. 6, pp. 1168–1173.

Jessberger, H. L. and Onnich, K., 1994, "Determination of Pollutant Transport Parameters by Laboratory Testing, *Proceedings, XIII International Conference on Soil Mechanics and Foundation Engineering,* New Delhi, India, pp. 1547–1552.

Katchalsky, A. and Curran, P. F., 1965, *Nonequilibrium Thermodynamics in Biophysics,* Harvard University Press, Cambridge, MA.

Keijzer, Th. J. S., Kleingeld, P. J., and Loch, J. P. G., 1997, "Chemical Osmosis in Compacted Clayey Material and the Prediction of Water Transport," *Geoenvironmental Engineering, Contaminated Ground: Fate of Pollutants and Remediation,* R. N. Yong and H. R. Thomas, Eds., University of Wales, Cardiff, U.K., 6–12 Sept. Thomas Telford Publisher, London, pp. 199–204.

Kemper, W. D. and Quirk, J. P., 1972, "Ion Mobilities and Electric Charge of External Clay Surfaces Inferred from Potential Differences and Osmotic Flow," *Soil Science Society of America Proceedings,* Vol. 36, pp. 426–433.

Kemper, W. D. and Rollins, J. B., 1966, "Osmotic Efficiency Coefficients Across Compacted Clays," *Soil Science Society of America Proceedings,* Vol. 30, pp. 529–534.

Koerner, R. M., 1994, *Designing with Geosynthetics,* 3rd ed., Prentice-Hall, Englewood Cliffs, NJ.

Letey, J., Kemper, W. D., and Noonan, L., 1969, "The Effect of Osmotic Pressure Gradients on Water Movement in Unsaturated Soil," *Soil Science Society of America Proceedings,* Vol. 33, pp. 15–18.

Marine, I. W. and Fritz, S. J., 1981, "Osmotic Model to Explain Anomalous Hydraulic Heads," *Water Resources Research,* Vol. 17, No. 1, pp. 73–82.

Mitchell, J. K., 1993, *Fundamentals of Soil Behavior,* 2nd ed., John Wiley and Sons, New York.

Olsen, H. W., 1969, "Simultaneous Fluxes of Liquid and Charge in Saturated Kaolinite," *Soil Science Society of America Proceedings,* Vol. 33, pp. 338–344.

Olsen, H. W., 1972, "Liquid Movement Through Kaolinite Under Hydraulic, Electric, and Osmotic Gradients," *American Association of Petroleum Geologists Bulletin,* Vol. 56, No. 10, pp. 2022–2028.

Olsen, H. W., 1985, "Osmosis: A Cause of Apparent Deviations from Darcy's Law," *Canadian Geotechnical Journal,* Vol. 22, pp. 238–241.

Olsen, H. W., Nichols, R. W., and Rice, T. L., 1985, "Low Gradient Permeability Measurements in a Triaxial System," *Geotechnique,* Vol. 35, No. 2, pp. 145–157.

Olsen, H. W., Yearsley, E. N., and Nelson, K. R., 1990, "Chemico-Osmosis Versus Diffusion-Osmosis," *Transportation Research Record No. 1288,* Transportation Research Board, Washington, DC, pp. 15–22.

Olsen, H. W., Gill, J. D., Willden, A. T., and Nelson, K. R., 1991, "Innovations in Hydraulic-Conductivity Measurements," *Transportation Research Record No. 1309,* Transportation Research Board, Washington, DC, pp. 9–17.

Redmond, P. L. and Shackelford, C. D., 1994, "Design and Evaluation of a Flow Pump System for Column Testing," *Geotechnical Testing Journal,* Vol. 17, No. 3, pp. 269–281.

Shackelford, C. D., 1991, "Laboratory Diffusion Testing for Waste Disposal - A Review," *Journal of Contaminant Hydrology,* Vol. 7, No. 3, pp. 177–217.

Shackelford, C. D., 1993, "Contaminant Transport," Chap. 3, *Geotechnical Practice for Waste Disposal,* D. E. Daniel, Ed., Chapman and Hall, London, pp. 33–65.

Shackelford, C. D. and Daniel, D. E., 1991, "Diffusion in Saturated Soil: I. Background," *Journal of Geotechnical Engineering,* ASCE, Vol. 117, No. 3, pp. 467–484.

Shackelford, C. D. and Redmond, P. L., 1995, "Solute Breakthrough Curves for Processed Kaolin at Low Flow Rates," *Journal of Geotechnical Engineering,* ASCE, Vol. 121, No. 1, pp. 17–32.

Shackelford, C. D., Benson, C. H., Katsumi, T., Edil, T. B., and Lin, L., 2000, "Evaluating the Hydraulic Conductivity of GCLs Permeated with Non-Standard Liquids," *Geotextiles and Geomembranes,* Elsevier, Amsterdam, Vol. 18, Nos. 2/3, pp. 133–161.

Shackelford, C. D., Malusis, M. A., Majeski, M. J., and Stern, R. T., 1999, "Electrical Conductivity Breakthrough Curves," *Journal of Geotechnical and Geoenvironmental Engineering,* ASCE, Vol. 125, No. 4, pp. 260–270.

Staverman, A. J., 1951, "Non-Equilibrium Thermodynamics of Membrane Processes," *Transactions of the Faraday Society,* Vol. 48, No. 2, pp. 176–185.

Van Oort, E., Hale, A. H., Mody, F. K., and Roy, S., 1996, "Transport in Shales and the Design of Improved Water-based Shale Drilling Fluids," *SPE Drilling and Completion,* Society of Petroleum Engineers, Vol. 11, No. 3, pp. 137–146.

Yeung, A. T., 1990, "Coupled Flow Equations for Water, Electricity and Ionic Contaminants Through Clayey Soils Under Hydraulic, Electrical, and Chemical Gradients," *Journal of Non-Equilibrium Thermodynamics,* Vol. 15, pp. 247–267.